Feature Article:

Cancer diagnosis and analysis devices based on multimolecular crowding

Daisuke Onoshima[1, *] and Yoshinobu Baba[1-3]

1. Institute of Nano-Life-Systems, Institutes of Innovation for Future Society, Nagoya University, Furo-cho, Chikusa-ku, Nagoya 464-8601, Japan
2. Department of Biomolecular Engineering, Graduate School of Engineering, Nagoya University, Furo-cho, Chikusa-ku, Nagoya 464-8603, Japan
3. Institute of Quantum Life Science, Quantum Life and Medical Science Directorate, National Institutes for Quantum Science and Technology (QST), Anagawa 4-9-1, Inage-ku, Chiba, 263-8555, Japan

*Corresponding author
E-mail: onoshima-d@nanobio.nagoya-u.ac.jp

Abstract

The study of the multimolecular crowding around cancer cells has opened up the possibility of developing new devices for cancer diagnosis and analysis through the measurement of intercellular communication related to cell proliferation and invasive metastasis associated with cancer malignancy. In particular, cells and extracellular vesicles that flow into the bloodstream contain metabolites and secreted products of the cancer microenvironment. These are positioned as targets for the development of new devices for the understanding and application of multimolecular crowding around cancer cells. Examples include the separation analysis of cancer cells in blood for the next generation of less invasive testing techniques, and mapping analysis using Raman scattering to detect cancer cells without staining. Another example is the evaluation of the relationship between exosomes and cancer traits for the exploration of new anti-cancer drugs, and the commercialization of exosome separation devices for ultra-early cancer diagnosis. The development of nanobiodevice engineering, which applies multimolecular crowding to conventional nanobioscience, is expected to contribute to the diagnosis and analysis of various diseases in the future.

1. Introduction

Cancer often refers to a tumor with a dense aggregation of cancer cells, but there are structures in tumors called stroma that are different from cancer cells [1]. In the stroma, pericytes isolated from blood vessel walls and fibroblasts that constitute connective tissue form characteristic structures [2]. These are called the "cancer microenvironment" (Fig. 1). In the cancer microenvironment, many metabolic products and secretory products form a crowding environment around cancer cells [3]. This environment causes cell dysfunction and abnormal tissue morphology due to intercellular communication that is different from normal.

Multimolecular crowding in the cancer microenvironment has long been a focus of research in the field of cancer pathology. Factors that promote the formation of blood vessels and lymph vessels [4], or inflammatory cytokines [5] have been examined. In recent years, the therapeutic effects of inhibitors targeting immune checkpoint molecules in cancer cells have been attracting attention [6-8], and thus an understanding of the cancer microenvironment is strongly required in the field of cancer immunotherapy [9,10].

Chronic inflammation is one of the most prominent pathologies observed in the cancer microenvironment [11,12]. Chronic inflammation refers to the chronic state of fibrosis, angiogenesis, and accumulation of certain immune cells in the inflammatory site [13]. This condition is a common underlying pathology in chronic diseases such as metabolic syndrome [14]. For example, bioactive substances secreted by hypertrophic fat cells cause inflammation in blood vessels and organs during obesity [15]. Inflammatory responses are generally considered to have a pro-tumor effect that promotes tumorigenesis and an anti-tumor effect that opposes tumorigenesis [16]. The pro-tumor effect is strongly observed in the cancer microenvironment. When the pro-inflammatory cytokine TNF-α is secreted, the signal induces the secretion of other cytokines such as interleukins [17] and the activation of the carcinogenic transcription factor NF-κB [18-20]. This turns on the oncogenic switch. In addition, various factors secreted by the cancer cells themselves recruit macrophages and immature bone marrow cells to induce invasion, malignant transformation, and metastasis of the cancer cells [21].

The diverse characteristics of the cancer microenvironment are distinguished by the type of cancer. Kidney cancers are richly vascularized [22]. Pancreatic cancers generate a large number of fibroblasts [23]. In gliomas, which are highly malignant brain tumors, the glioma cells themselves secrete the cytokine TGF-β [24]. TGF-β was first identified as a

tumor suppressor that inhibits cell proliferation, but it was later shown to convert epithelial cells into mesenchymal cells and to have a tumoricidal effect on non-epithelial cancers [25]. In addition, it has been tested to induce glioma cell differentiation by suppressing TGF-β signaling [26]. Thus, manipulating the molecular adulteration of the cancer microenvironment will allow us to explore the possibility of developing new cancer therapeutics.

In this feature article, we focus on the properties of cells and extracellular vesicles associated with the cancer microenvironment. The analysis of these cells and extracellular vesicles has been advanced by the development of devices for magnetic cell sorting [27,28], droplet analysis [29], circulating reactors [30], and thermophores [31]. These cells and extracellular vesicles contain metabolites and secreted products of the cancer microenvironment. Therefore, separation analysis of their membrane components and spectral analysis of their internalized components will expand the possibility of detecting components of the multimolecular crowding around cancer cells and developing devices based on multimolecular crowding. Here, we mainly describe the development of technology to obtain effective information for cancer diagnosis and analysis by measuring very small amounts of cancer-related cells flowing into the bloodstream and exosomes secreted outside the cells in the process of intercellular communication, as well as practical examples of clinical applications. In the outlook, we will discuss the possibility of nanobiodevice research to analyze multimolecular crowding by constructing a cancer microenvironment on a device chip.

2. Separation analysis of cancer cells in blood

Small amounts of cancer-related cells are present in the peripheral blood of cancer patients, including cancer cells with the ability to metastasize to other sites (circulating tumor cells: CTCs) [32] and fibroblasts in the cancer microenvironment [33]. It is not yet clear whether CTCs are biomarkers of hematogenous metastasis or the cause of metastasis itself, but analysis of CTCs has proven to be very useful at least for prognostic monitoring to rapidly track drug resistance and hematogenous metastatic potential of tumors with changing characteristics [34]. In many cases, the applicability of cancer chemotherapy is determined by the presence or absence of metastases [35]. Since the diagnosis has a significant impact on the prognosis, the measurement of CTC is an important indicator to determine the correct treatment strategy [36].

In the field of cancer diagnosis, tissue biopsy is the most reliable method for obtaining definitive results [37], especially when the importance of disease prognosis is considered. However, tissue biopsy has to be performed with caution because it is highly invasive and can lead to serious complications. For example, in chronic renal failure, renal biopsy is the definitive diagnosis [38] that determines whether dialysis is indicated, but the rate of this procedure is very low. Ovarian, prostate, kidney, lung, and pancreas cancers are also known to be difficult to biopsy [39,40]. Therefore, a number of measurement methods are being investigated to overcome the challenges of tissue biopsy by making it possible to detect cancer diagnostic markers such as CTCs in blood in minute amounts, at high speed, and with high accuracy. This method is called "liquid biopsy" [41-43] as it replaces the conventional tissue biopsy with a blood test.

The U.S. Food and Drug Administration has approved a CTC detection device [44] that automates the process of separating CTCs by the magnetic force of anti-EpCAM antibody-modified magnetic particles against epithelial cell adhesion molecule (EpCAM) on the surface of CTCs. The number of CTCs in 7.5 mL of blood is counted after immunological and nucleic acid staining operations. Recently, a new technique has been developed to isolate and subsequently culture CTCs by filtration of blood [45]. This technique (Fig. 2) is called ISET (Isolation by Size of Epithelial Tumor cells), which utilizes the fact that the size of CTCs differs from that of white blood cells (WBCs) and red blood cells (RBCs) [46]. For example, a CTC detection kit that combines a vacuum blood collection tube and a polycarbonate membrane filter has been commercialized [47]. When 10 mL of blood is passed through the filter, which has a pore size of 8 μm and 45,000 pores, CTCs are separated in about 3 minutes. The separated CTCs can be transferred to a microtiter plate or dish with the filter and used for culture tests. A CTC detection system combining a syringe pump and a membrane filter made of SU-8, a light-curing resin, has also been commercialized [48]. The high processing accuracy and pore density of the lithography technology achieves a pore diameter of 7 μm and a pore number of 160,000. The time required to pass blood through the filter has been reduced to about 50 seconds.

The author's research group has been working on the development of a lab-on-a-chip for the separation and analysis of CTCs using a microfabricated membrane separation filter [49-51]. In addition to using the pores as a filter for size separation [52], we are developing an application that aims to capture a single CTC in one pore (Fig. 3) and use

it as a function to realize subsequent genetic analysis. This will enable diagnosis to select molecular targeted drugs and immune checkpoint inhibitors from blood tests. It is also expected to increase the possibility of receiving appropriate treatment in a less invasive manner according to the stage and type of cancer.

In order to detect cancer cells by fluorescence, it is necessary to stain cell nuclei and membrane proteins with dyes. For example, it is often reported [53,54] that antibodies conjugated with dyes are applied to EpCAM on the surface of CTCs. On the other hand, there are cancer cells that do not have EpCAM on their surface. To address this issue, Raman spectroscopy has recently been studied to detect cancer cells without staining. Raman spectroscopy has been mainly used for the characterization of solid substrates [55]. However, it has many optical advantages that can also be used for the analysis of biological materials [56]. For example, the versatility, rapidity, non-contact, and non-destructive advantages of Raman spectroscopy may be useful for the detection of biological components in cells [57]. Raman spectra are affected by several parameters such as the number and concentration of biomolecules [58]. Therefore, measuring the Raman spectrum of a single cell can identify the cell type without additional labeling of the cell [59]. The author's research group has measured the Raman spectra of cancer cells at the single cell level [60]. Analysis of the fingerprint region of the Raman spectrum (1,200 cm-1 to 1,800 cm-1) using confocal Raman microscopy allows mapping of cancer cells in a pattern specific to amide bonds (Fig. 4).

3. Cancer traits and exosomes

The phenomenon of cells secreting nano-sized vesicles into the extracellular space has been observed in almost all cells including bacteria [61-64]. As an example of intercellular communication [65], physiological studies have been accelerated to elucidate the formation process, release mechanism, and internal dynamics of extracellular vesicles. In particular, exosomes, which are characterized by nucleic acids, lipids, proteins, and other components encapsulated in vesicles, are well known [66]. Recent studies [67,68] have reported the phenomenon that cancer cells secrete more exosomes than normal cells. It has also been pointed out that exosomes are involved in the maintenance of cancer traits [69]. For example, a group of tyrosine kinases is responsible for intracellular signaling, and regulates cell proliferation and invasive metastasis associated with malignant transformation of cancer. Some of the molecules

that intervene in this signaling are involved in the production mechanism of exosomes. Furthermore, exosomes secreted by cancer cells contain microRNAs that communicate with surrounding cells [66,70]. Clarifying the factors that reduce the ability of cancer cells to produce exosomes will open up the possibility of cancer treatment using new anticancer drugs.

In the area of practical research for clinical application of exosomes as disease-specific biomarkers, exosomes have been evaluated by detection of membrane proteins [71-73]. Enzyme-linked immunosorbent assay (ELISA) is often used to detect these membrane proteins [74-76]. This has led to the development of test tools that can process multiple samples simultaneously. There is a report [77] on the use of an ELISA-based exosome detection tool to detect exosomal membrane proteins in the plasma of melanoma patients. In this report, plasma samples from 90 melanoma patients and 58 healthy subjects were used. Exosomes were collected by ultracentrifugation, and membrane proteins such as Rab5b and caveolin-1 were detected. Progress has also been made in developing new, higher throughput detection systems. For example, there is a method [78] of sandwiching the membrane proteins of exosomes between two monoclonal antibodies with different modifications. The unique feature of this technique is that it detects fluorescence that occurs only when two antibodies are within 200 nm of each other. This technique has been successfully used to detect exosomal membrane proteins such as CD63 and CD9 in 5 μL of healthy human serum using each antibody. On the other hand, body fluids also contain many proteins that are different from those derived from exosomes [79-81]. They may interfere with the targeted reaction of the exosome detection tool. In addition, insufficient amounts of exosomes may prevent the required detection sensitivity from being achieved, so significant progress is still expected in the development of exosome purification and enrichment tools.

4. Exosome separation devices

The ultracentrifugation method [82-84] has been used to isolate exosomes for a long time, but it is not suitable for processing a large number of samples because of its complicated and time-consuming operation. Furthermore, it has been reported [85] that the amount of exosomes isolated by ultracentrifugation tends to be low. The ultracentrifugation method involves a long period of ultrahigh-speed centrifugation, and some exosomes may have been damaged by physical stress. Equilibrium density gradient

centrifugation [82,84,86] is used to increase the degree of purification in ultracentrifugation. A high degree of purification can be obtained if the sample is centrifuged with density gradient solute and the corresponding density fraction is collected exactly each time. However, it has a drawback that it is difficult to achieve reproducibility in multi-specimen processing.

The immunological capture method utilizes antibodies specific for antigens on the surface of exosomes and collects exosomes by binding them to various carriers. For example, a kit containing CD9, CD63, CD81, and EpCAM antibodies conjugated to magnetic beads of several micrometers in diameter has been commercialized [87]. In addition, a column of antibodies coated on a spin-tube type filter [88,89] can capture exosomes by low-speed centrifugation. Exosome enrichment is achieved by repeatedly adding samples. However, the pattern of antigens expressed on the surface of exosomes varies among producing cells and tissues. It should be noted that the immunological capture method specifically enriches exosomes that express many specific surface antigens.

The size-exclusion method is the easiest way to obtain high-purity exosomes. By setting a gel filtration column to HPLC and subjecting the sample to size exclusion chromatography, exosomes can be recovered as fractions that elute faster than soluble proteins [90]. On the other hand, the size-exclusion method tends to have a low degree of purification because it depends only on the size of the particles. Therefore, column products using packing materials that combine the size exclusion method with weak hydrophobic interactions have been developed [91]. This column is a tool to fractionate exosomes from other proteins and lipoproteins by using the difference in surface hydrophobicity in addition to particle size. The author's research group has also studied glass filters that have developed separation properties for exosomes using a well-controlled porous structure [92,93]. In this study, the possibility of new size separation beyond the conventional size exclusion effect has been investigated by utilizing the characteristics of the interconnected pores. In addition, multifaceted verification including the effect of surface modification is in progress. For example, a coating agent that enhances the separation of proteins from glass filters with nano-sized porous structures in spin columns is being tested. The preparation conditions of the coating solution and the immersion agitation conditions of the glass filter were experimentally verified. The results show that the amount of nonspecific adsorption of protein can be

reduced by more than 80% without pore blockage or appearance change. This has led to the successful capture of exosomes from plasma samples. The exosomes on the glass surface have been confirmed by electron microscopy and Raman spectroscopy (Fig. 5).

Other tools based on protein-polymer precipitation methods [94,95] are commercially available for exosome isolation, purification and enrichment. Some bead products targeting membrane components of exosomes bind to phosphatidylserine in the presence of metal ions. The addition of chelating agents enables elution of exosomes without dissolving them [92,96]. There is no end to the number of exosome purification and enrichment tools that continue to be developed.

5. Outlook

The analytical and applied chemistry of multimolecular crowding enables the creation of new biodevices for highly sensitive analysis of biological environments. Here, we reviewed specific examples such as separation analysis of cancer cells in blood, spectral analysis of cancer cells, cancer traits and exosomes, detection tools for exosomes, and separation devices for exosomes. In the future, it is important to develop molecular recognition tools for pericellular metabolites and extracellular vesicles. The development of cell-anchored DNA and aptamer sensors [97] is a good example.

Furthermore, it is important to develop nanobiodevices for analyzing complex multimolecular crowding. The analysis of multimolecular crowding in cancer microenvironment is a unique nano-bioscience in the interdisciplinary fields of materials engineering, analytical chemistry, and oncology. Although mass cytometers [98-100] and multicolor flow cytometers [101,102] can analyze cell surface markers and transcription factors, they are not suitable for the analysis of intercellular communication. The number of molecules to be measured is also limited. In addition, single-cell analysis using next-generation sequencers [103-105] is effective for studying the cancer immune microenvironment, but it has issues with cost and throughput.

In contrast, nanobiodevices have the characteristic of being able to construct multimolecular crowding in the pathological environment of cancer, which makes them unique and original from conventional research. For example, it is possible to construct a cancer microenvironment on a microfabricated device chip and use artificial intelligence to analyze the molecular impurity information obtained by fluorescence imaging and Raman spectroscopy. This is expected to elucidate the diversity of the cancer immune

microenvironment, as represented by the interaction between immune checkpoint molecules and inhibitors. It is also expected that the analytical and applied chemistry of multimolecular crowding can be applied to the study of cancer mechanisms.

The advancement of nanobiodevice research is expected to lead to the development of molecular environment devices for artificial cells and synthetic biology, tissue engineering and regenerative medicine devices as typified by Organ on a Chip, molecular analysis devices that integrate machine learning and deep learning, novel drug discovery devices for the development of molecular targeted drugs for cancer, and treatment devices for the lifestyle-related diseases. The results of these developments are also expected to be applied to IoT sensors.

Conflicts of interest

There are no conflicts to declare.

Acknowledgements

This work was supported by a Grant-in-Aid for Scientific Research on Innovative Areas "Chemistry for Multimolecular Crowding Biosystems" (JSPS KAKENHI Grant No. JP 17H06354)

References

1. D. Hanahan, R. A. Weinberg, Cell, 2011, 144, 646-674.
2. D. M. Gilkes, G. L. Semenza, D. Wirtz, Nat. Rev. Cancer, 2014, 14, 430-439.
3. M. J. Bissell, W. C. Hines, Nat. Med., 2011, 17, 320-329.
4. B. Mlecnik, G. Bindea, A. Kirilovsky, H. K. Angell, A. C. Obenauf, M. Tosolini, S. E. Church, P. Maby, A. Vasaturo, M. Angelova, T. Fredriksen, S. Mauger, M. Waldner, A. Berger, M. R. Speicher, F. Pagès, V. V.-Archer, J. Galon, Sci. Transl. Med., 2016, 8, 327ra26.
5. P. Berraondo, M. F. Sanmamed, M. C. Ochoa, I. Etxeberria, M. A. Aznar, J. L. Pérez-Gracia, M. E Rodríguez-Ruiz, M. P.-Sarvise, E. Castañón, I. Melero, Br. J. Cancer, 2019, 120, 6-15.
6. Y. Cao, X. Wang, T. Jin, Y. Tian, C. Dai, C. Widarma, R. Song, F. Xu, Signal Transduct Target Ther., 2020, 5, 250.
7. Y. Yu, X. Ma, Y. Zhang, Y. Zhang, J. Ying, W. Zhang, Q. Zhong, A. Zhou, Y. Zeng, J. Cancer, 2019, 10, 2754-2763.
8. L. Sams, S. Kruger, V. Heinemann, D. Bararia, S. Haebe, S. Alig, M. Haas, D. Zhang, C. B. Westphalen, S. Ormanns, P. Metzger, J. Werner, O. Weigert, M. von B.-Baildon, F. Rataj, S. Kobold, S. Boeck, Clin. Transl. Oncol. 2021, 23, 2394-2401.
9. J. D. Wolchok, T. A. Chan, Nature, 2014, 515, 496-498.
10. G. Kroemer, L. Galluzzi, O. Kepp, L. Zitvogel, Annu. Rev. Immunol., 2013, 31, 51-72.
11. L. M. Coussens, Z. Werb, Nature, 2002, 420, 860-867.
12. F. R. Greten, S. I. Grivennikov, Immunity, 2019, 51, 27-41.
13. G. Landskron, M. De la Fuente, P. Thuwajit, C. Thuwajit, M. A. Hermoso, J. Immunol. Res., 2014, 2014, 149185.
14. J. V. Forrester, L. Kuffova, M. Delibegovic, Front Immunol., 2020, 11, 583687.
15. N. M. Iyengar, A. Gucalp, A. J. Dannenberg, C. A. Hudis, J. Clin. Oncol., 2016, 34, 4270-4276.
16. A. J. Ozga, M. T. Chow, A. D. Luster, Immunity, 2021, 54, 859-874.
17. S. W. Coppack, Proc. Nutr. Soc., 2001, 60, 349-356.
18. A. B. Kunnumakkara, B. Shabnam, S. Girisa, C. Harsha, K. Banik, T. B. Devi, R. Choudhury, H. Sahu, D. Parama, B. L. Sailo, K. K. Thakur, S. C. Gupta, B. B. Aggarwal, Crit. Rev. Immunol., 2020, 40, 1-39.

19. B. B. Aggarwal, Y. Takada, S. Shishodia, A. M. Gutierrez, O. V. Oommen, H. Ichikawa, Y. Baba, A. Kumar, Indian J. Exp. Biol., 2004, 42, 341-353.
20. R. Ralhan, M. K. Pandey, B. B. Aggarwal, Front Biosci., 2009, 1, 45-60.
21. J. Caers, E. Van Valckenborgh, E. Menu, B. Van Camp, K. Vanderkerken, Bull Cancer, 2008, 95, 301-313.
22. S. K. Lau, R. Klein, Z. Jiang, L. M. Weiss, P. G. Chu, Hum. Pathol., 2010, 41, 1500-1504.
23. H. Sadozai, A. Acharjee, S. E.-Castori, B. Gloor, T. Gruber, M. Schenk, E. Karamitopoulou, Front Immunol., 2021, 12, 643529.
24. A. Sasaki, H. Naganuma, E. Satoh, T. Kawataki, K. Amagasaki, H. Nukui, Neurol. Med. Chir., 2001, 41, 253-258.
25. B. Kaminska, M. Kocyk, M. Kijewska, Adv. Exp. Med. Biol., 2013, 986, 171-187.
26. A. W. Nana, P. M. Yang, H. Y. Lin, Asian Pac. J. Cancer Prev., 2015, 16, 6813-6823.
27. R. M. Mohamadi, J. D. Besant, A. Mepham, B. Green, L. Mahmoudian, T. Gibbs, I. Ivanov, A. Malvea, J. Stojcic, A. L. Allan, L. E. Lowes, E. H. Sargent, R. K. Nam, S. O. Kelley, Angew. Chem. Int. Ed. Engl., 2015, 54, 139-143.
28. L. Kermanshah, M. Poudineh, S. Ahmed, L. N. M. Nguyen, S. Srikant, R. Makonnen, F. P. Cantu, M. Corrigan, S. O. Kelley, Lab Chip, 2018, 18, 2055-2064.
29. T. Schneider, J. Kreutz, D. T. Chiu, Anal. Chem., 2013, 85, 3476-3482.
30. X. Zhou, H. Cao, Y. Zeng, Talanta, 2021, 232, 122396.
31. Y. Li, J. Deng, Z. Han, C. Liu, F. Tian, R. Xu, D. Han, S. Zhang, J. Sun, J. Am. Chem. Soc., 2021, 143, 1290-1295.
32. H. J. West, J. O. Jin, JAMA Oncol., 2015, 1, 394.
33. Z. Ao, S. H. Shah, L. M. Machlin, R. Parajuli, P. C. Miller, S. Rawal, A. J. Williams, R. J. Cote, M. E. Lippman, R. H. Datar, D. El-Ashry, Cancer Res., 2015, 75, 4681-4687.
34. J. C. Fischer, D. Niederacher, S. A. Topp, E. Honisch, S. Schumacher, N. Schmitz, L. Z. Föhrding, C. Vay, I. Hoffmann, N. S. Kasprowicz, P. G. Hepp, S. Mohrmann, U. Nitz, A. Stresemann, T. Krahn, T. Henze, E. Griebsch, K. Raba, J. M. Rox, F. Wenzel, C. Sproll, W. Janni, T. Fehm, C. A. Klein, W. T. Knoefel, N. H. Stoecklein, Proc. Natl. Acad. Sci. USA, 2013, 110, 16580-16585.
35. I. J. Fidler, M. L. Kripke, Cancer Metastasis Rev., 2015, 34, 635-641.
36. E. S. Lianidou, A. Markou, Clin. Chem., 2011, 57, 1242-1255.

37. F. J. Frassica, E. F. McCarthy, D. A. Bluemke, Instr. Course Lect., 2000, 49, 437-442.
38. J. Bandari, T. W. Fuller, R. M. T. Ii, L. A. D'Agostino, Can. J. Urol., 2016, 23, 8121-8126.
39. K. F.-Dyer, A. Ahmad, S. S. Arora, G. Wile, Abdom. Radiol., 2016, 41, 706-719.
40. R. S. Arellano, M. Maher, D. A. Gervais, P. F. Hahn, P. R. Mueller, 2003, 32, 218-226.
41. B. A.-Ardekani, P. Vielh, Acta Cytol., 2014, 58, 574-581.
42. Chiara Mannelli, Bioeth. Inq., 2019, 16, 551-557.
43. J. J. Nieva, P. Kuhn, Future Oncol., 2012, 8, 989-998.
44. S. Riethdorf, H. Fritsche, V. Müller, T. Rau, C. Schindlbeck, B. Rack, W. Janni, C. Coith, K. Beck, F. Jänicke, S. Jackson, T. Gornet, M. Cristofanilli, K. Pantel, Clin. Cancer Res., 2007, 13, 920-928.
45. M. M. Ferreira, V. C. Ramani, S. S. Jeffrey, Mol. Oncol., 2016, 10, 374-394.
46. J. M. Kwan, Q. Guo, D. L. Kyluik-Price, H. Ma, M. D. Scott, Am. J. Hematol., 2013, 88, 682-689.
47. M. Ilie, V. Hofman, E. L.-Mira, E. Selva, J.-M. Vignaud, B. Padovani, J. Mouroux, C.-H. Marquette, P. Hofman, PLoS One, 2014, 9, e111597.
48. D. L. Adams, S. Stefansson, C. Haudenschild, S. S. Martin, M. Charpentier, S. Chumsri, M. Cristofanilli, C.-M. Tang, R. K. Alpaugh, Cytometry A, 2015, 87, 137-144.
49. D. Onoshima, D. Kuboyama, N. Kihara, H. Tanaka, T. Hase, H. Yukawa, K. Ishikawa, H. Odaka, Y. Hasegawa, M. Hori, Y. Baba, Proc. Micro Total Analysis Systems ’18, 2018, 1291-1293.
50. N. Kihara, H. Odaka, D. Kuboyama, D. Onoshima, K. Ishikawa, Y. Baba, M. Hori, Jpn. J. Appl. Phys., 2018, 57, 037001.
51. N. Kihara, D. Kuboyama, D. Onoshima, K. Ishikawa, H. Tanaka, N. Ozawa, T. Hase, R. Koguchi, H. Yukawa, H. Odaka, Y. Hasegawa, Y. Baba, M. Hori, Jpn. J. Appl. Phys., 2018, 57, 06JF03.
52. D. Onoshima, H. Yukawa, Y. Hattori, K. Ishikawa, M. Hori, Y. Baba, Proc. Micro Total Analysis Systems ’17, 2017, 679-680.

53. A. Kuske, T. M. Gorges, P. Tennstedt, A.-K. Tiebel, R. Pompe, F. Preißer, S. Prues, M. Mazel, A. Markou, E. Lianidou, S. Peine, C. A.-Panabières, S. Riethdorf, B. Beyer, T. Schlomm, K. Pantel, Sci. Rep., 2016, 6, 39736.
54. H.-Y. Chu, L.-S. Lu, W. Cho, S.-Y. Wu, Y.-C. Chang, C.-P. Lin, C.-Y. Yang, C.-H. Lin, J.-K. Jiang, F.-G. Tseng, Cancers, 2019, 11, 56.
55. D. L. Gerrard, Anal. Chem., 1994, 66, 547R-557R.
56. H. J. Butler, L. Ashton, B. Bird, G. Cinque, K. Curtis, J. Dorney, K. E.-White, N. J. Fullwood, B. Gardner, P. L. M.-Hirsch, M. J. Walsh, M. R. McAinsh, N. Stone, F. L. Martin, Nat. Protoc., 2016, 11, 664-687.
57. A. Germond, V. Kumar, T. Ichimura, J. Moreau, C. Furusawa, H. Fujita, T. M. Watanabe, J. R. Soc. Interface, 2017, 14, 20170174.
58. K. Eberhardt, C. Stiebing, C. Matthäus, M. Schmitt, J. Popp, Expert Rev. Mol. Diagn., 2015, 15, 773-787.
59. A. J. Hobro, Y. Kumagai, S. Akirac, N. I. Smith, Analyst, 2016, 141, 3756-3764.
60. D. Onoshima, K. Uchida, H. Yukawa, K. Ishikawa, M. Hori, and Y. Baba, Proc. Micro Total Analysis Systems ’19, 2019, 1374-1375.
61. G. van Niel, G. D'Angelo, G. Raposo, Nat. Rev. Mol. Cell. Biol., 2018, 19, 213-228.
62. E. R. Abels, X. O. Breakefield, Cell Mol. Neurobiol., 2016, 36, 301-312.
63. F. Cocozza, E. Grisard, L. M.-Jaular, M. Mathieu, C. Théry, Cell, 2020, 182, 262-262.e1.
64. S. Bose, S. Aggarwal, D. V. Singh, N. Acharya, Microb. Cell., 2020, 7, 312-322.
65. O. Stegle, S. A. Teichmann, J. C. Marioni, Nat. Rev. Genet., 2015, 16, 133-145.
66. D. K. Jeppesen, A. M. Fenix, J. L. Franklin, J. N. Higginbotham, Q. Zhang, L. J. Zimmerman, D. C. Liebler, J. Ping, Q. Liu, R. Evans, W. H. Fissell, J. G. Patton, L. H. Rome, D. T. Burnette, R. J. Coffey, Cell, 2019, 177, 428-445.e18.
67. L. Zhang, D. Yu, Biochim. Biophys. Acta Rev. Cancer, 2019, 1871, 455-468.
68. A. Gonda, J. Kabagwira, G. N. Senthil, N. R. Wall, Mol. Cancer Res., 2019, 17, 337-347.
69. A. Becker, B. K. Thakur, J. M. Weiss, H. S. Kim, H. Peinado, D. Lyden, Cancer Cell, 2016, 30, 836-848.
70. D. D. Taylor, C. G.-Taylor, Gynecol. Oncol., 2008, 110, 13-21.
71. C. He, S. Zheng, Y. Luo, B. Wang, Theranostics, 2018, 8, 237-255.

72. J. Lin, J. Li, B. Huang, J. Liu, X. Chen, X.-M. Chen, Y.-M. Xu, L.-F. Huang, X.-Z. Wang, ScientificWorldJournal, 2015, 2015, 657086.
73. Q. Hu, H. Su, J. Li, C. Lyon, W. Tang, M. Wan, T. Y. Hu, Precis. Clin. Med., 2020, 3, 54-66.
74. C. Göhner, M. Weber, D. S. Tannetta, T. Groten, T. Plösch, M. M. Faas, S. A. Scherjon, E. Schleußner, U. R. Markert, J. S. Fitzgerald, Am. J. Reprod. Immunol., 2015, 73, 582-588.
75. F. A. W. Coumans, E. L. Gool, R. Nieuwland, Platelets, 2017, 28, 242-248.
76. S. M. Moghimi, I. Hamad, J. Liposome Res., 2008, 18, 195-209.
77. M. Logozzi, A. De Milito, L. Lugini, M. Borghi, L. Calabrò, M. Spada, M. Perdicchio, M. L. Marino, C. Federici, E. Iessi, D. Brambilla, G. Venturi, F. Lozupone, M. Santinami, V. Huber, M. Maio, L. Rivoltini, S. Fais, PLoS One, 2009, 4, e5219.
78. Y. Yoshioka, N. Kosaka, Y. Konishi, H. Ohta, H. Okamoto, H. Sonoda, R. Nonaka, H. Yamamoto, H. Ishii, M. Mori, K. Furuta, T. Nakajima, H. Hayashi, H. Sugisaki, H. Higashimoto, T. Kato, F. Takeshita, T. Ochiya, Nat. Commun., 2014, 5, 3591.
79. N. Karimi, A. Cvjetkovic, S. C. Jang, R. Crescitelli, M. A. H. Feizi, R. Nieuwland, J. Lötvall, C. Lässer, Cell Mol. Life Sci., 2018, 75, 2873-2886.
80. J.-Y. Choi, S. Kim, H.-B. Kwak, D.-H. Park, J.-H. Park, J.-S. Ryu, C.-S. Park, J.-H. Kang, Int. Neurourol. J., 2017, 21, 83-96.
81. H. K. Skalnikova, B. Bohuslavova, K. Turnovcova, J. Juhasova, S. Juhas, M. Rodinova, P. Vodicka, Proteomes, 2019, 7, 17.
82. D. W. Greening, R. Xu, H. Ji, B. J. Tauro, R. J. Simpson, Methods Mol. Biol., 2015, 1295, 179-209.
83. C. Coughlan, K. D. Bruce, O. Burgy, T. D. Boyd, C. R. Michel, J. E. G.-Perez, V. Adame, P. Anton, B. M. Bettcher, H. J Chial, M. Königshoff, E. W. Y. Hsieh, M. Graner, H. Potter, Curr. Protoc. Cell Biol., 2020, 88, e110.
84. S. Gupta, S. Rawat, V. Arora, S. K. Kottarath, A. K. Dinda, P. K. Vaishnav, B. Nayak, S. Mohanty, Stem Cell Ther., 2018, 9, 180.
85. L. Cheng, X. Sun, B. J. Scicluna, B. M. Coleman, Andrew. F. Hill, Kidney Int., 2014, 86, 433-444.
86. R. J. Lobb, M. Becker, S. W. Wen, C. S. F. Wong, A. P. Wiegmans, A. Leimgruber, A. Möller, J. Extracell. Vesicles, 2015, 4, 27031.

87. R. S. Patel, G. Carter, G. E. Bassit, A. A. Patel, D. R. Cooper, M. Murr, N. A. Patel, Stem Cell Investig., 2016, 3, 2.
88. Y. Sato, S. Ochiai, T. Murata, T. Kanda, F. Goshima, H. Kimura, Oncotarget, 2017, 8, 39345-39355.
89. S. Tsuda, M. Shinohara, T. Oshita, M. Nagao, N. Tanaka, T. Mori, T. Hara, Y. Irino, R. Toh, T. Ishida, K. Hirata, Sci. Rep., 2017, 7, 12989.
90. J. D. Arroyo, J. R. Chevillet, E. M. Kroh, I. K. Ruf, C. C. Pritchard, D. F. Gibson, P. S. Mitchell, C. F. Bennett, E. L. P.-Agadjanyan, D. L. Stirewalt, J. F. Tait, M. Tewari, Proc. Natl. Sci. USA, 2011, 108, 5003-5008.
91. S. Sjoqvist, K. Otake, Y. Hirozane, Int. Mol. Sci., 2020, 21, 9425.
92. K. Aoki, H. Yukawa, D. Onoshima, S. Yamazaki, N. Kihara, R. Koguchi, K. Takahashi, H. Odaka, K. Ishikawa, M. Hori, Y. Baba, Proc. Micro Total Analysis Systems ’18, 2018, 1409-1410.
93. H. Yukawa, S. Yamazaki, K. Aoki, K. Muto, N. Kihara, K. Sato, D. Onoshima, T. Ochiya, Y. Tanaka, Y. Baba, Sci. Rep., 2021, 11, 8672.
94. T. Tomiyama, G.-X. Yang, M. Zhao, W. Zhang, H. Tanaka, J. Wang, P. S. C. Leung, K. Okazaki, X.-S. He, Q. Lu, R. L. Coppel, C. L. Bowlus, M. E. Gershwin, Cell. Mol. Immunol., 2017, 14, 276-284.
95. R. E. Lane, D. Korbie, W. Anderson, R. Vaidyanathan, M. Trau, Sci. Rep., 2015, 5, 7639.
96. S. Muraoka, M. P. Jedrychowski, K. Yanamandra, S. Ikezu, S. P. Gygi, T. Ikezu, Cells, 2020, 9, 1959.
97. W. Zhao, S. Schafer, J. Choi, Y. J. Yamanaka, M. L. Lombardi, S. Bose, A. L. Carlson, J. A. Phillips, W. Teo, I. A. Droujinine, C. H. Cui, R. K. Jain, J. Lammerding, J. C. Love, C. P. Lin, D. Sarkar, R. Karnik, J. M. Karp, Nat. Nanotechnol., 2011, 6, 524-531.
98. P. Maby, A. Corneau, J. Galon, Methods Enzymol., 2020, 632, 339-368.
99. C. Giesen, H. A. O. Wang, D. Schapiro, N. Zivanovic, A. Jacobs, B. Hattendorf, P. J. Schüffler, D. Grolimund, J. M. Buhmann, S. Brandt, Z. Varga, P. J. Wild, D. Günther, B. Bodenmiller, Nat. Methods, 2014, 11, 417-422.
100. B. Korin, T. Dubovik, A. Rolls, Nat. Protoc., 2018, 13, 377-391.
101. A. Galvin, M. Weglarz, K. F.-Donahue, M. Handley, M. Baum, M. Mazzola, H. Litwa, D. T. Scadden, L. Silberstein, Curr. Protoc. Cytom., 2019, 87, e50.

102. J. F. van Velzen, B. A. P. L.-van Gorkom, G. A. M. Pop, W. L. van Heerde, Thromb. Res., 2012, 130, 92-98.
103. N. Murphy, P. Shah, A. Shih, H. Khalili, A. Liew, X. Zhu, A. Lee, Adv. Exp. Med. Biol., 2020, 1255, 153-164.
104. M. Singer, A. C. Anderson, Cancer Immunol. Res., 2019, 7, 168-173.
105. Y. Xu, G.-H. Su, D. Ma, Y. Xiao, Z.-M. Shao, Y.-Z. Jiang, Signal Transduct. Target Ther., 2021, 6, 312.

Figures and captions

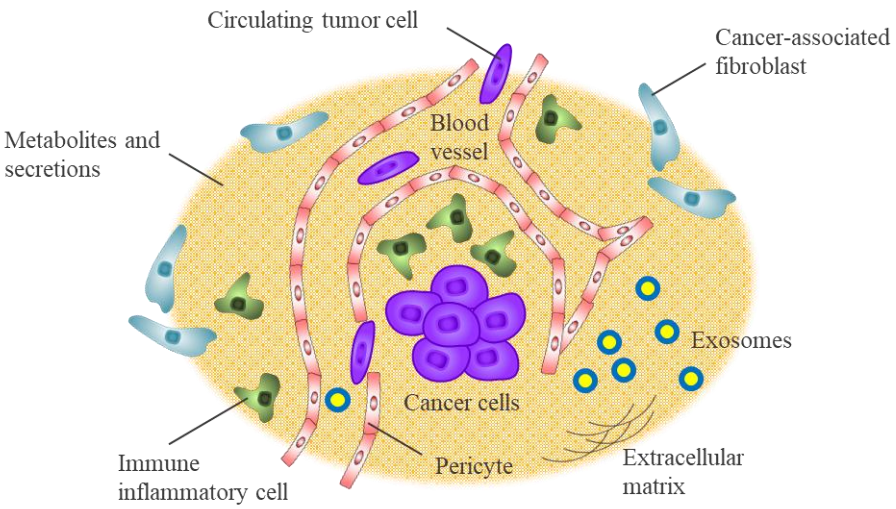

Fig. 1. Schematic of the cancer microenvironment.

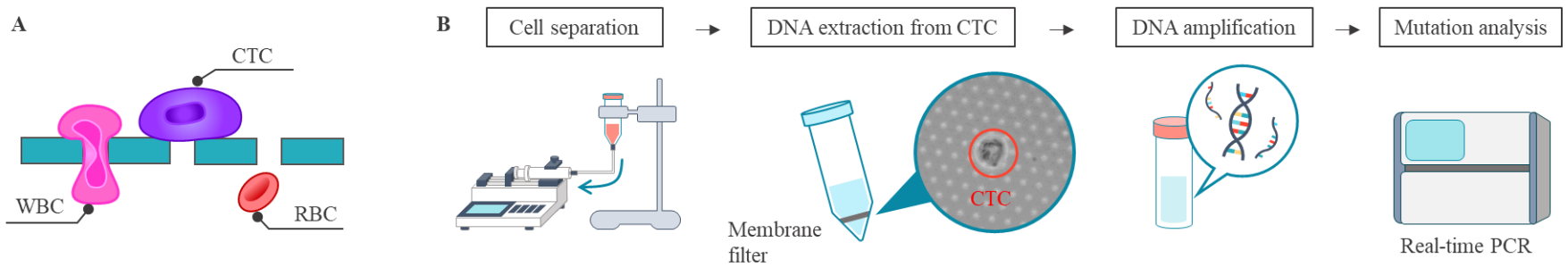

Fig. 2. ISET principles and protocols for downstream analysis. A: Conceptual diagram of CTC's size separation filter. CTCs and WBCs are separated by microfilters due to differences in cell stiffness and plasticity; CTCs are less rigid than normal cells and more rigid than WBCs [46]. B: Flow of genetic mutation analysis for CTCs. DNA extracted from CTCs is measured by real-time PCR with whole genome amplification or partial sequence amplification. In particular, genetic mutations to epidermal growth factor receptor (EGFR) are detected for the purpose of analyzing drug resistance in tumors [45]. All figure data were prepared and modified based on ref. 49.

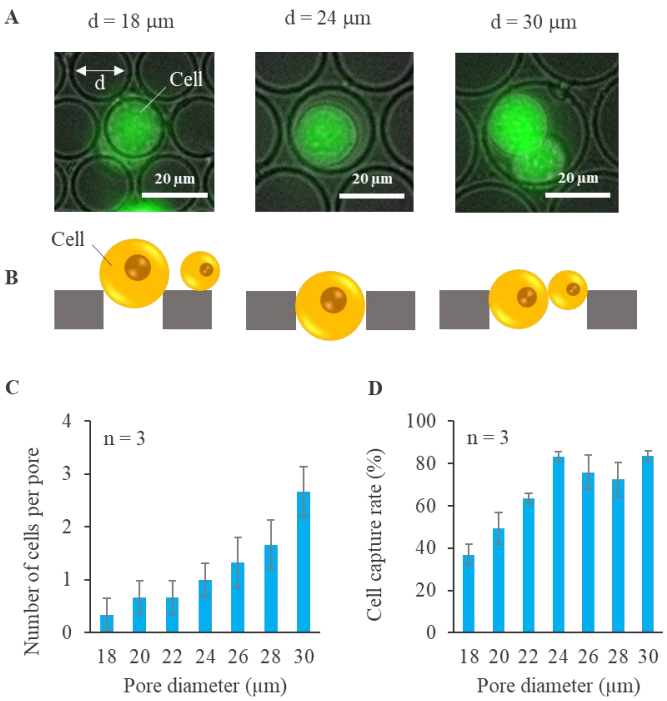

Fig. 3. Development of micropore filters for single cell capture. A: Fluorescence microscopy images of cells trapped in micropores. In the microchannel, the cell line MCF-7 was trapped in micropores at the bottom of the channel. The diameter of MCF-7 was 13-24 µm. MCF-7 was stained with Calcein-AM. The number of trapped cells depended on the pore size (d) of the micropore. B: Conceptual diagram showing the state of cell capture (side view). C: Relationship between number of cells per pore and pore diameter. The data show the mean and standard deviation of three measurements. D: Relationship between cell capture rate and pore diameter. The data show the mean and standard deviation of three measurements. All figure data were prepared and modified based on ref. 52.

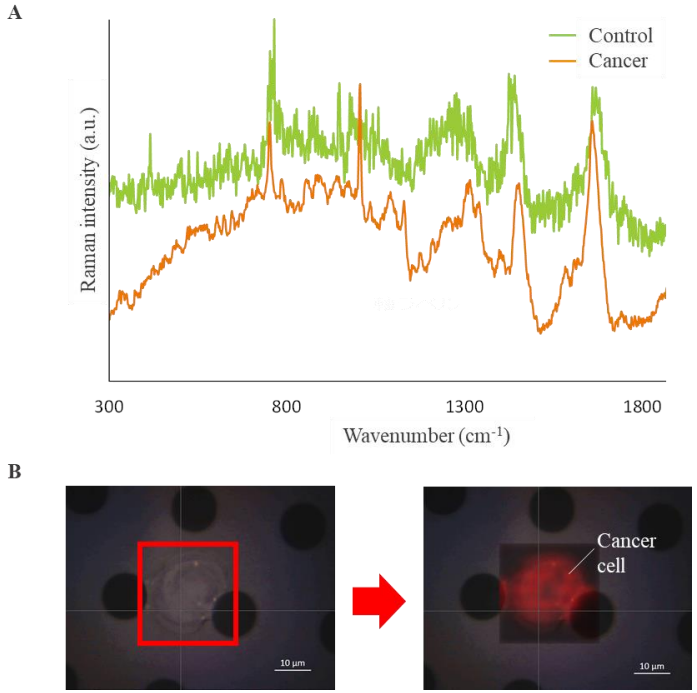

Fig. 4. Examples of Raman scattering light measurements of cells. A: Raman spectra of cancer cells and control cells. The Raman spectrum of the cancer cells shows the measurement of the cell line H358. Excitation wavelength of 532 nm was used. The Raman spectrum of the control cells shows the averaged data of non-cancer cell lines. B: Mapping measurement of a cancer cell by Raman scattering light. Cell image of H358 was mapped using the peak attributed to amide bonds. All figure data were prepared and modified based on ref. 60.

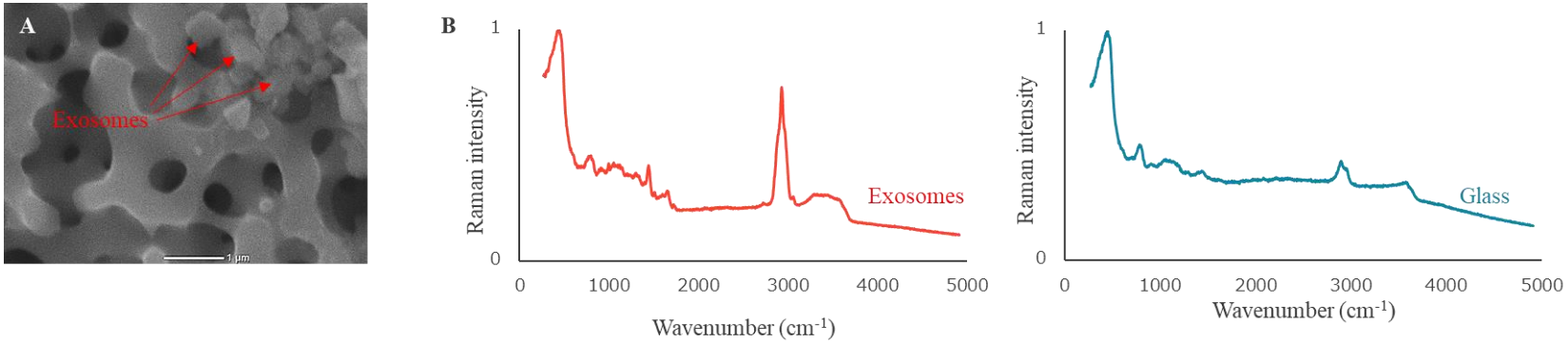

Fig. 5. Example of Raman scattering light measurement of exosomes. A: Electron microscopy image of exosomes trapped on a glass filter. B: Normalized Raman spectra of exosomes and glass filter. Excitation wavelength of 532 nm was used. Exosomes were collected from the supernatant of the cell line HepG2 by centrifugation on the glass filter and measured directly. The Raman spectrum of exosomes showed characteristic peaks attributed to C-N, C-O, and C-H bonds. All figure data were prepared and modified based on ref. 92.